J. Fluid Mech. (1974), *vol.* 63, *part* 2, *pp.* 315–343
Printed in Great Britain

An investigation of the topography and motion of the turbulent interface

By S. T. PAIZIS AND W. H. SCHWARZ
Department of Mechanics and Materials Science, The Johns Hopkins University

(Received 24 January 1973)

The sharp interface which exists in unbounded turbulent shear flows was studied using a linear array of twenty hot-wire probes. The probe arrangement was such that the location of the interface could be monitored instantaneously. The particular flow examined was a two-dimensional turbulent wall jet. It was found that the interface is a highly contorted surface which exhibits a significant amount of folding. Quantitative methods for characterizing this behaviour are presented, together with pertinent measurements. In addition, measurements of the mean surface area of the interface, and space–time corrrelations of the width of the turbulence were obtained. The latter were used to find characteristic scales and convection velocities of the interface.

1. Introduction

1.1. *Nature of the investigation*

A very striking feature of unbounded turbulent shear flows is the very sharp demarcation that exists between the turbulent motion and the surrounding non-turbulent region. This interface, apparently found in all such flows, entrains non-turbulent fluid as it advances into the ambient region. Its motion is random, both in space and time. Why such a sharp boundary of the turbulent flow should exist is not fully understood, although it seems clear that it is a result of the nonlinear character of the equations that govern turbulent motions.

This investigation concerned itself with a number of aspects of the turbulent interface. The primary aim was to study the topography and motion of the interface, to find ways of characterizing its features and to measure some of its properties. The approach was experimental, the results serving to motivate various concepts, and forming a basis for the analytical description of the interface. The experimental method centred around an array of hot-wire probes which served to locate the interface, thereby providing measures of its statistical properties. The particular turbulent flow examined was the two-dimensional plane wall jet.

1.2. *Survey of previous work*

The turbulent interface and the flow occurring in its vicinity have been the subject of a number of studies since Corrsin (1943) first observed that the output of a hot-wire probe had an intermittent character when placed in the outer region of a jet flow. Townsend (1948, 1949) introduced the concept of the intermittency factor: the fraction of time that the flow at any point is turbulent. He measured

this quantity in a wake flow and used it to infer properties of the turbulent part of the flow.

The first detailed study of the turbulent interface was by Corrsin & Kistler (1955). This classic work shed much light on the nature of the interface and the associated entrainment process. The mean position and standard deviation of the interface at a number of downstream locations were measured in a rough-wall boundary layer and round jet, and it was found that these properties grew as the characteristic flow width. The probability distribution of the interface location was determined to be closely normal. It was argued on dimensional grounds that the propagation speed and thickness of the interface should be determined by the viscosity and the mean-square vorticity in the vicinity of the interface. Finally, they concluded that the non-turbulent region is a field of irrotational motion, so that the interface is in fact a layer across which the vorticity drops to zero.

Numerous studies related to the properties of the interface followed this work. An analysis of the irrotational motion by Phillips (1955) predicted that the intensity of the irrotational velocity fluctuations should fall to zero as the fourth power of the distance from some point in the flow. This result has been confirmed on a number of occasions: most recently by Kovasznay, Kibens & Blackwelder (1970) in a boundary layer, and by Wygnanski & Fiedler (1970) in a mixing layer. The latter also verified an additional result of Phillips, that the mean-square value of the velocity fluctuations normal to the plane of the interface equals the sum of those in the transverse directions.

Some impressive experimental methods for studying the intermittent region were devised by Kovasznay *et al.* (1970). Based on the intermittency function, which is unity if the flow at a point is turbulent and zero otherwise, they could measure flow properties during turbulent (or non-turbulent) periods alone. Mean velocities in the two zones in a boundary layer were measured and found to differ by as much as 6%. Local convection velocities of the interface were measured to be about 7% less than the free-stream velocity. In addition they measured point averages, whereby a flow variable was sampled only when the interface was at some specific location. From these and many other results a very elaborate representation of the 'average' flow in the vicinity of an 'average' turbulent bulge was inferred (Blackwelder & Kovasznay 1972*b*). Through space–time correlation measurements of velocity and the intermittency function, it was established that the shape of the interface is intimately related to the large-scale turbulent motions.

This idea had been proposed earlier by Townsend (1956), who postulated that the large eddies of the turbulence contorted the interface thereby controlling the rate of entrainment of ambient fluid. Based on visual observation of wake flows (Townsend 1966), he suggested that the interface undergoes a growth and decay cycle during which rapid entrainment occurs, followed then by a quiescent period. Modelling the turbulence as an elastic fluid and the irrotational motion as that of an inviscid fluid, a stability analysis showed that the initially planar interface was unstable to disturbances below a critical wavenumber.

The idea that the turbulent flow can exhibit an elastic character was found by

Moffatt (1965) in a study of the response of a weak turbulence to a uniform shearing motion. He discovered that the mean velocity was governed by a wave equation, with a wave speed proportional to the square root of the kinetic energy of the weak fluctuations. The non-uniformity of this kinetic energy led to a discontinuity of the mean velocity and to a propagation of this discontinuity.

Townsend (1970) argued that, since the rate of entrainment was set by the structural similarity of the flow, the entrainment process would have to adjust itself to satisfy this rate. The large differences in entrainment rates between wakes and boundary layers suggested that the entrainment processes might differ in these flows. The lack of any periodicity in the boundary-layer interface (Kovasznay *et al.* 1970) as compared with the cyclic behaviour of the wake interface were pointed out as illustrations of these differences.

Assuming a constant propagation velocity of the interface, Phillips (1972) studied the kinematics of surfaces in some simple flows. It was found that, if the convective component of the fluid velocity was less than the propagation velocity, discontinuities would develop in the slope of the surface and relatively rapid entrainment would result. The converse situation led to a comparatively inactive behaviour of the surface and lower entrainment speeds. Phillips then went on to interpret the result of Kovasznay *et al.* (1970) in the light of these findings, suggesting that it is the slower moving eddies that are responsible for the entrainment of ambient fluid.

No rigorous explanation for the existence of the interface has yet been given. Corrsin & Kistler (1955) proposed that the stretching of vortex lines in the presence of a local gradient in vorticity leads to a steepening of this gradient since the rate of production of vorticity is proportional to the vorticity present. An analysis of the vorticity equation averaged over short times supported this argument. Although Moffatt (1965) has criticized this idea, pointing out that the rate of destruction of vorticity is also proportional to the vorticity present, it must be close to the truth.

Recently, phenomenological theories describing turbulent flows have included the interface (e.g. Nee & Kovasznay 1969; Saffman 1970; Lundgren 1970). The aim in these is to impart some structure to the interface, and properties such as the mean thickness and propagation velocity are sought. All assume a planar interface, which is unstable to large-scale wave disturbances according to an analysis of Reynolds (1972).

The cornerstone of the experimental study of the turbulent interface has been the intermittency function mentioned above. This function is constructed from the output of a hot-wire probe by appropriate electronic operations. The original circuit was constructed by Townsend (1949) and has been elaborated and improved upon since then, the most recent being a very elegant circuit used by Kohan (1968). Modern techniques have included the use of digital computers for the analysis of the probe outputs (Coles & Van Atta 1967; Kaplan & Laufer 1969). Kaplan & Laufer used an array of ten probes to study the intermittent region of a turbulent boundary layer. The probes were calibrated, so the system was capable of monitoring the location of the interface as well as the motion in its neighbourhood.

2. Experimental methods

The major experimental tool used in this study was a linear array of twenty hot-wire probes which, coupled with anemometers and detector circuits, served to locate the position of the turbulent interface. The probes used were Thermo-Systems Model 1276 subminiature probes with tungsten hot-wire sensors. The probes were mounted on a brass rod, with spacings of 0·467 cm ($\frac{3}{16}$ in.): see figure 1.

The outputs of the constant-temperature anemometers associated with these probes were fed into turbulence (intermittency) detector circuits whose function was to produce an output which was 'on' (1) if the probe was in a turbulent field and 'off' (0) otherwise. These outputs were available for processing to determine properties of the interface. The first operation was to add all these outputs in a summing amplifier. This sum gives the width of the turbulence passing the rake. Another measure was constructed by counting the number of consecutive probes that 'saw' turbulence, the counting being started from the probe closest to the fully turbulent region. This was accomplished by using logic circuitry. The final operation (the crossing circuit) was to count the number of changes of 'state' that occurred along the rake. Consecutive detector outputs were compared in 'exclusive or' gates whose outputs were 'on' only if the inputs differed, i.e. only if an interface crossing was detected. The number of 'on' signals occurring at any instant was equal to the number of times that the interface intersected the probe rake. The arrangement is shown schematically in figure 1, where for clarity only five channels are included.

For single-point measurements of the intermittency function a Thermo-Systems Model 1274 boundary-layer probe and Model 1010 constant-temperature anemometer were used with a turbulence detector circuit much like the ones associated with the hot-wire rake. The same type of probe and anemometer together with a Thermo-Systems Model 1010 Linearizer were used to measure velocities.

Spatial correlations were determined by analog multiplication followed by an integration, while temporal correlations were computed using a P.A.R. Model 100 Correlator. The mean values of the signals being correlated were removed by using blocking capacitors in all cases, the low-frequency cut-off being 0·017 Hz. Complete details of all the above procedures are given by Paizis (1972).

The measurements were undertaken in a two-dimensional wall jet. The wall jet is described by Paizis (1972) and Kohan (1968), where gross features of the development of the flow are also reported.

The detection of turbulence is a subjective procedure in which the output of the sensor, usually a single hot-wire probe, is suitably processed, e.g. differentiated and rectified, and then compared with some preset gate level. If this level is exceeded the flow is considered turbulent. The level is usually set on a trial and error basis, comparing the gate input to the output and adjusting the gate level until the two signals are reasonably matched.

For the probe rake twenty gate levels must be set independently. If the probes were calibrated then this operation would be considerably simplified for the

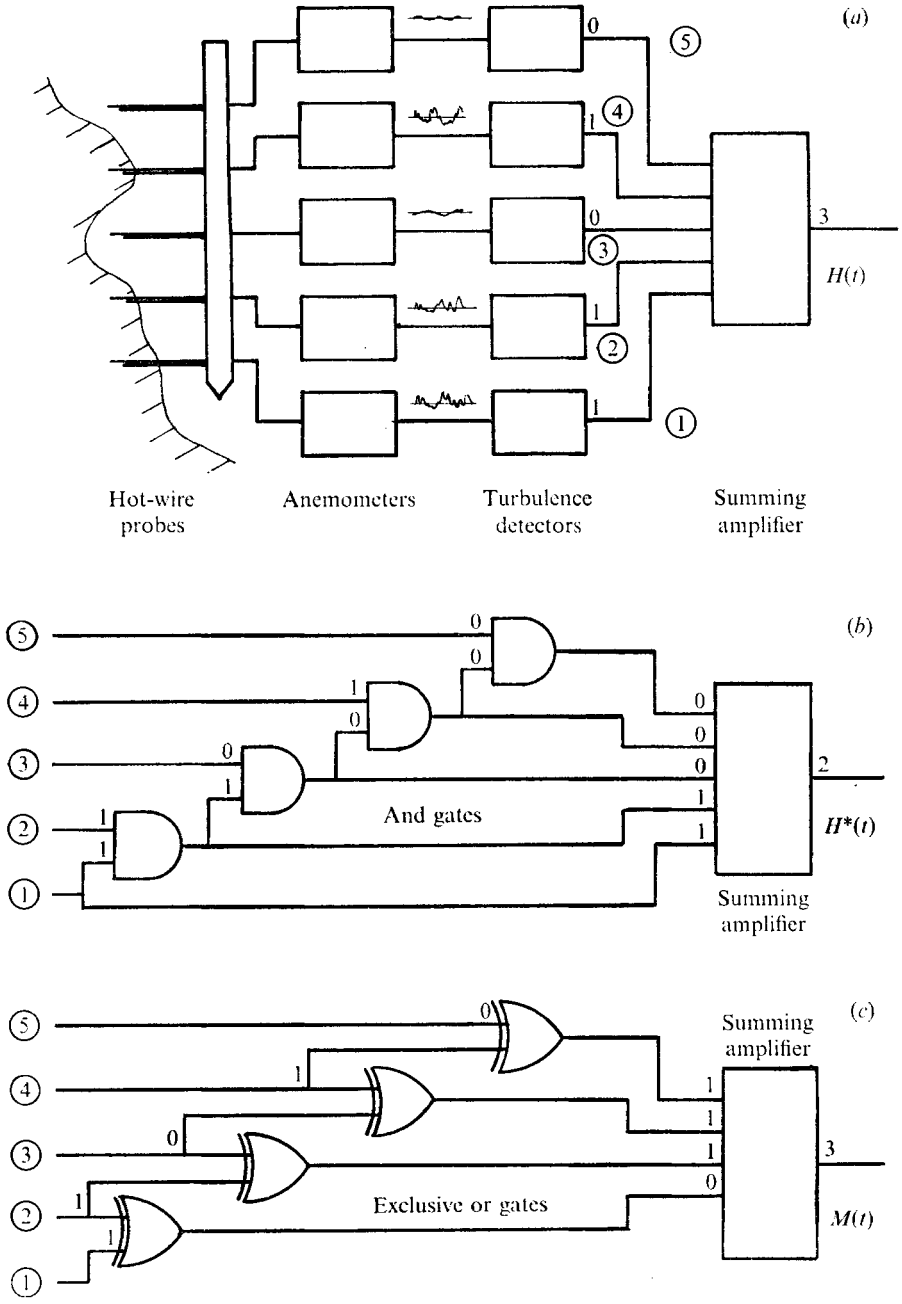

FIGURE 1. (*a*) The hot-wire rake and associated electronics. Only five channels are shown for clarity. (*b*) Counting circuit. (*c*) Crossing circuit.

gates could be set consistently as some function of the turbulence level. Unfortunately calibration of the probes was not feasible. It is difficult to predict what the effect of a mismatch in the gate settings has on the various operations described above. Whatever the effect is, the summing amplifier will tend to average out the errors that may arise. This is not so for the other two circuits.

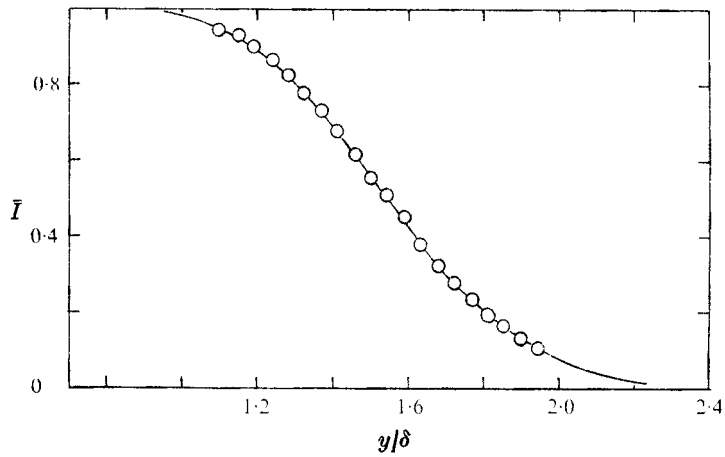

FIGURE 2. Intermittency factor profiles: ——, from single-wire traverse; ○, from hot-wire rake outputs.

The counting circuit is sensitive to one particular gate setting at any time (that one which detects the first interface crossing), while the crossing circuit is effectively a differentiator and so will be more susceptible to errors due to a gate mismatch.

Great care was taken in setting the gate levels. The procedure adopted was as follows. The rake was placed in the intermittent region with the downstream distance chosen such that the rake spanned approximately four standard deviations of the interface position. The gate levels were then set individually and an intermittency factor profile measured. This was compared with a profile determined by a single-wire traverse, then the gate levels were finely readjusted to bring these two profiles into close agreement (figure 2). The final test that was made was to determine the probability density of the interface. This was done by comparing the outputs of two adjacent detector outputs and computing the fraction of time that the signals differed, using an 'exclusive on' gate. The probability density function was measured first by using the full rake and next by traversing with the first two probes on the rake. These results are shown in figure 3. The agreement is very good so the rake can be used with confidence, for it reproduces the probability density of the interface, and it is from this function that almost all of its statistical properties emerge.

The next question that arises concerns the finite spacing of the probes. The interface is tracked to within one probe spacing by the rake. This is equivalent to $0{\cdot}044\delta$, where δ is the boundary-layer thickness at the position where the measurements were made, and since the range of the interface location is of order δ, the interface is located with an accuracy of about 5 %.

The rake acts as a spatial filter, for no variations in the interface position of scale less than the probe spacing will be detected. Using the Corrsin & Kistler (1955) dimensional argument and the dissipation measurements of Wygnanski & Fiedler (1969), the thickness of the interface is estimated to be of the order of $0{\cdot}001\delta$. Thus, there is a range of scales from $0{\cdot}04\delta$ to $0{\cdot}002\delta$ which will not be

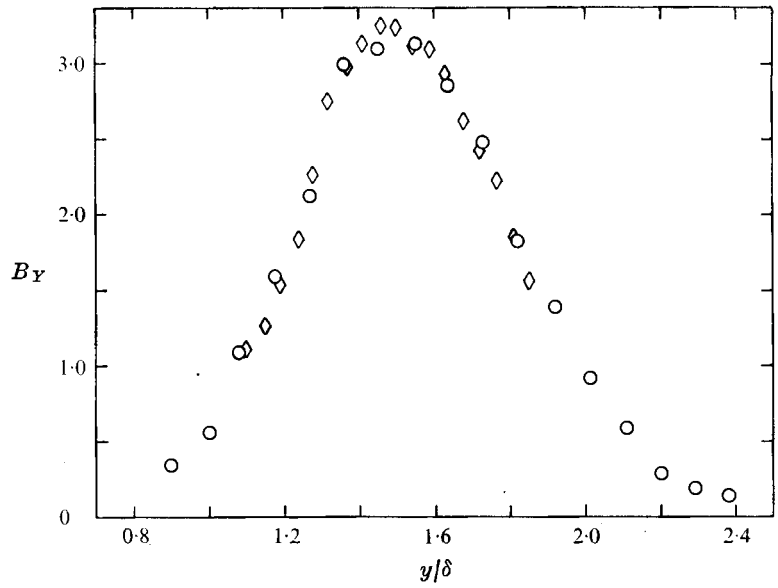

FIGURE 3. Probability density of the interface position: ○, from two-wire traverse; ◇, from hot-wire rake outputs.

susceptible to measurement. This information is lost anyway, since in the detection of the interface it is necessary to discard pulses from the detector outputs which are less than a certain width (the drop-out problem is discussed by Paizis 1972). It turns out that this width (3 μs) corresponds to scales of order $0{\cdot}03\delta$.

3. Geometry of the interface

3.1. *The character of the turbulent interface*

Experimental evidence for the existence of the interface arises primarily from two sources. The observation of the intermittent character of the output of a hot-wire probe when placed in the flow suggests that there is a sharp distinction between the turbulent flow and the ambient fluid, the latter exhibiting only large-scale fluctuations in velocity. Visualization of the flow by various means indicates that there is a continuous surface which completely surrounds the turbulent flow.

Consequently, it seems reasonable to describe the interface as a surface in the flow field, and it can be conveniently represented by the equation

$$y = Y(x, z, t),$$

where Y is a smooth positive-valued random function of x, z and t. Envisioned is a flow with the x co-ordinate being the direction of the main flow, and y the inhomogeneous direction. It will be assumed throughout that $Y(x,z,t)$, and indeed all properties of the interface, are homogeneous functions of x and z, and stationary in t. This simplifies the study of its statistical properties enormously. To account for the variation of the mean properties with downstream distance

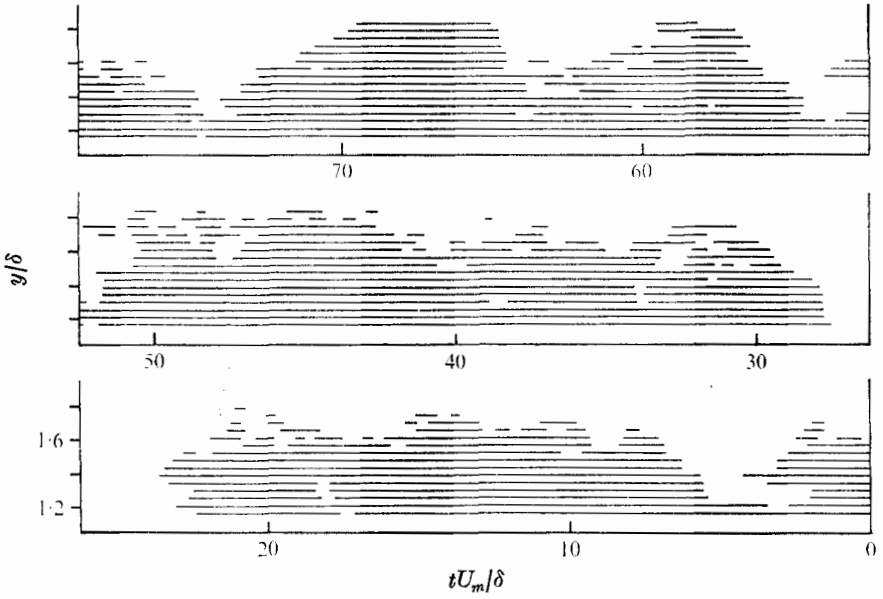

FIGURE 4. Oscillograph traces of hot-wire rake outputs. Solid line represents the presence of turbulence.

all such properties will be normalized with suitable combinations of local length and velocity scales.

Recalling the definition of the intermittency function $I(x, y, z, t)$ as being unity when the flow at a point is turbulent and zero otherwise, it can be equated to an indicator function

$$\Phi(x, y, z, t) = \begin{cases} 1 & \text{if} \quad Y \geqslant y, \\ 0 & \text{if} \quad Y < y \end{cases}$$

if and only if $Y(x, z, t)$ is a single-valued function of its variables. Assuming that this is in fact so, it follows that

$$Y = \int_0^\infty I \, dy,$$

and Y can be approximated by the finite sum

$$Y = \sum_{i=1}^{N} I(y_i)\,(y_{i+1} - y_i).$$

Thus, if a sufficient number of probes, whose outputs were proportional to $I(t)$, spanned the range of the interface position, their sum would be a good approximation to $Y(t)$. To get some idea of the interface shape, the hot-wire rake was placed in the wall jet flow, 360 slot widths downstream of the jet exit. The detector outputs were recorded on a multi-channel oscillograph and a sample trace is shown in figure 4.

There are a number of features of these traces that are worth noting. The interface is not a smoothly wrinkled sheet, but rather a highly contorted surface. The isolated patches of turbulence are most probably parts of turbulent regions located to the side of the rake. In fact, an isolated turbulent region cannot exist

for, if such a region did depart from the bulk of the turbulence, it would still be connected to the main turbulent fluid by a thin region of vortical fluid.

The converse situation, that of the apparent 'holes' in the turbulent regions, could be indentations in the sides of turbulent bulges or they could be isolated regions of non-turbulent fluid. Such a situation is not impossible; indeed Townsend (1966, 1970) suggested that engulfing of ambient fluid by turbulence is the primary mechanism of entrainment. The trace in figure 4, although it does not support such an idea, does not rule it out either.

The turbulent bulges are not symmetrical. The fronts (leading edges) appear to be steeper than the backs (trailing edges). The backs display a diffuse character, there being much folding in these regions, while the fronts are sharp and relatively free of these isolated and overhanging regions.

It is interesting to compare this trace with the records of Kaplan & Laufer (1969) obtained in the intermittent region of a turbulent boundary layer. Their records of the outputs of 10 probes display features similar to those reported here. There are also some differences. They report that the leading edges are steeper, and while it does appear so, it is not as marked as in the wall jet. Also, the leading edges are the regions of ragged character. This is confirmed by the fascinating films of a smoke-filled boundary layer reported by Fiedler & Head (1966). The shape of the interface in a boundary layer is in a sense similar to that of a jet although the relative velocities are opposite, i.e. the boundary layer is a velocity defect flow, whereas the jet is one of velocity excess. The dye photographs in a wake by Grant (1958) and Townsend (1966) support this idea.

It is clear then that the interface position is not always a single-valued function. Some means of characterizing the extent to which this phenomenon occurs seems desirable, and this will be considered next.

3.2. *Measures of folding*

For those flows which contain a fully turbulent region, a formal definition of a fold can be given as follows: a fold is a region of turbulent fluid which has non-turbulent fluid between it and the fully turbulent region. Thus in figure 4 the apparently isolated turbulent patches (which are most probably parts of turbulent regions located to the side of the rake) are folds; as are the regions above the non-turbulent 'holes' and of course the overhanging portions of the turbulent bulges.

To characterize the interface position completely, two additional single-valued functions would be needed for each fold that occurs. On a more practical level, two functions will be used to describe the interface. The first, $H(x,z,t)$, is the total width of turbulent fluid at (x,z) at time t. This is easily measured as the sum of the turbulence detector outputs. The second function, $H^*(x,z,t)$, is the width of turbulent fluid that is not part of the folds. This is available as the output of the counting circuit.

The difference between these two functions $H-H^*$ is the total width of the folds. The mean value of this quantity was measured in the wall jet and found to be

$$\overline{H-H^*} = 0{\cdot}05\delta,$$

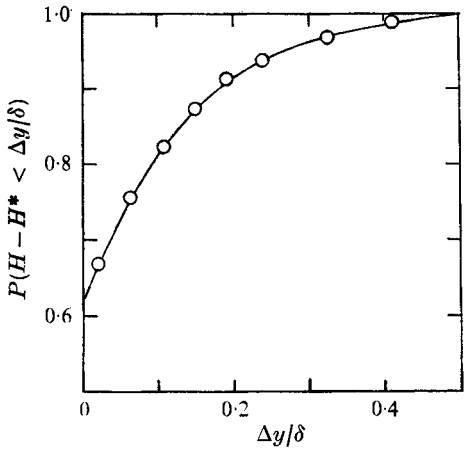

FIGURE 5. Probability distribution of folds.

where δ is the boundary-layer thickness. This does not constitute a large proportion of the total width of the turbulence, which is about $1{\cdot}5\delta$, but is more significant when compared with the standard deviation of the interface position, approximately $0{\cdot}3\delta$. These values are approximate for as yet we have not established measures for these properties.

The probability distribution of the function $H-H^*$ was measured and is shown in figure 5. It can be seen that folds occur about 40 % of the time, although they are usually of small width; folds with a total width equal to the standard deviation occur only with probability less than 0·05.

The extent to which folding occurs is significant, and, since the mean width of the turbulent fluid in the intermittent region is of order 2σ, it means that 10 % of this fluid will be carried in the folds. Probably most of it will be in regions above 'holes'. The many-valued character of the interface position is worthy of further study, but, since the standard techniques used for studying a random function fail when the function is many-valued, a new approach is needed to characterize the statistical properties of the interface position.

3.3. *Random multiple-valued functions*

Lumley (1964, 1970) presented a theory for the statistical properties of many-valued random functions, and it is this theory that will be followed. It is sufficient for our purposes to assume that the interface position Y takes on only a finite number of values at any time. Defining an indicator function as

$$\Psi(y,\Delta y) = \begin{cases} 1 & \text{if} \quad y \leqslant Y < y+\Delta y, \\ 0 & \text{otherwise}, \end{cases}$$

$\overline{\Psi}$ is the probability that Y takes on a value in the interval $[y, y+\Delta y)$. It will be assumed that the limit

$$\lim_{\Delta y \to 0} \overline{\Psi}/\Delta y = B_Y(y) \tag{1}$$

exists. B_Y is the probability density function of Y, but its integral

$$\int_0^\infty B_Y(y)\,dy$$

is not unity as is the case for single-valued functions. In fact, this integral defines the expected-valuedness of the function

$$M_Y = \int_0^\infty B_Y(y)\,dy.$$

The expected-valuedness can be interpreted as the zeroth moment of Y, and is the expected number of values that the function will take on.

The moments of Y are defined as

$$\overline{Y^n} = \int_0^\infty \frac{y^n B_Y(y)}{M_Y}\,dy.$$

As far as the single-point statistics of such a function are concerned, one can consider a sample of the function, remove any extra values it may take on, and add these on at the end of the sample. The moments of the resulting single-valued function can be computed and normalized with the expected-valuedness to account for the increase in sample length. This obviously cannot be done for multiple-point statistical properties, and although joint probability densities can be defined in the same way (Lumley 1964, 1970), their interpretation is difficult.

The probability density function was estimated by measuring $\overline{\Psi}$, using a two-wire traverse, as described in § 2, and applying (1). The result is shown in figure 3. The integral of this curve gives the expected-valuedness as $M_Y = 2{\cdot}35$. Since folding occurs with probability 0·4, the expected-valuedness in the folding region alone would be 4·4. This means that folds will not always occur singly.

3.4. *Statistical properties of the interface*

There are a number of possible ways of characterizing the statistical properties of the turbulent interface. It is desirable to define a mean position, a standard deviation and higher-order moments, and to extend these ideas to multiple-point properties, e.g. correlation coefficients.

(i) The first possibility is of course to use the theory of Lumley outlined in § 3.3. This would give true measures of the properties of the interface position, within the context of the theory. Measurements would need be done with two probes and, as mentioned above, multiple-point properties are not easily interpreted.

(ii) Properties measured by the conventional technique, viz. using the intermittency factor obtained by a single-wire traverse, have the advantage of being readily determined. Their significance is not clear when the interface position is many-valued, but they certainly do characterize the extent of the turbulent field.

(iii) The last possible measure to be considered is the width of the turbulent flow, the function $H(x, z, t)$ discussed earlier. Although only indirectly related to the interface position, it is probably more significant physically: it is this function which appears in the study of entrainment rates. Further, it is available as an analog signal (using the hot-wire rake), and its extension to multiple-point measurements is straightforward.

Some formal relationships between the three approaches can be derived. The probability density $B_Y(y)$ is related to the intermittency function by

$$B_Y(y) = \lim_{\Delta y \to 0} \frac{1}{\Delta y} [\overline{I(y+\Delta y)\{1-I(y)\} + I(y)\{1-I(y+\Delta y)\}}]$$
$$= \frac{\partial \bar{I}}{\partial y} - 2\left[\frac{\partial}{\partial y'} \overline{I(y)\, I(y')}\right]_{y'=y},$$

so two-point statistics of $I(y)$ are sufficient to determine $B_Y(y)$. An inverse relationship does not exist since $I(y)$ is not determined by Y, i.e. specification of Y does not establish whether the flow is turbulent at any point. Of course, I could be redefined as being unity at y if Y takes on an even number of values less than y. Then some relationship might exist, but it is not obvious just what it should be.

The width of the turbulent fluid H is directly related to I by

$$H = \int_0^\infty I(y)\, dy,$$

so a complete statistical description of I is needed (e.g. the characteristic functional), to determine the distribution of H. The mean values are equal, however, for

$$\bar{H} = \overline{\int_0^\infty I(y)\, dy} = \int_0^\infty \overline{I(y)}\, dy \equiv \bar{Y}_I.$$

No simple relationship exists for the standard deviations. In fact,

$$\sigma_H^2 = \int_0^\infty \int_0^\infty \overline{I(y)\, I(y')}\, dy\, dy' - \bar{H}^2$$

and

$$\sigma_I^2 = 2\int_0^\infty y \bar{I}(y)\, dy - \bar{Y}_I^2,$$

where the subscripts H and I refer to methods (iii) and (ii), respectively.

Probability distributions for the three approaches can be represented as

(i) $P(Y < y) = \int_0^y \frac{B_Y(y)}{M_Y}\, dy,$

(ii) $P(Y_I < y) = 1 - \bar{I}(y),$

(iii) $P(H < y).$

It should be stressed that the function Y_I has no physical significance if the interface position Y is multiple-valued. These three distributions have been calculated for the wall jet and are presented in figure 6. The similarity between $P(Y < y)$ and $1 - \bar{I}$ is striking and suggests that use of the intermittency factor profile as a representation of the probability distribution of the interface position is reasonable. It is not surprising that $P(H < y)$ differs from the other two, for in constructing $H(x, z, t)$, the Y function is compressed, valleys (regions of small Y) being filled with folds, thus leading to a smaller standard deviation. The mean values and standard deviations have been determined from these distributions, and are presented in table 1.

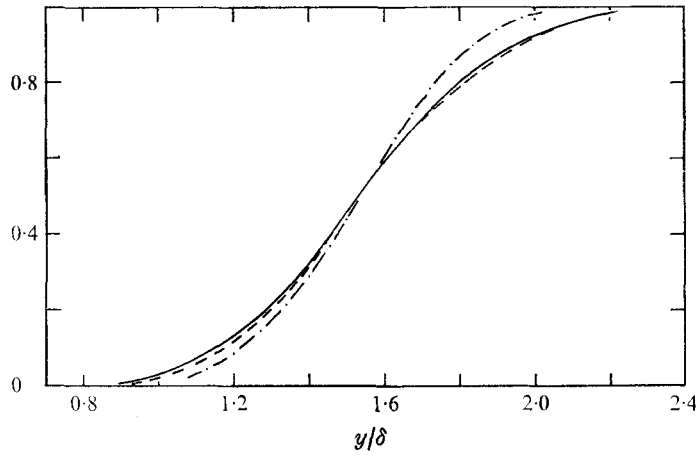

FIGURE 6. Probability distribution of the interface position: ——, $\int B_Y/M_Y d(y/\delta)$; – – –, $1-\bar{I}$; –·–·–, $P(H < y)$.

Method	Mean position	Standard deviation
(i) $Y(x, z, t)$	1·53	0·303
(ii) Y_I	1.55	0·280
(iii) $H(x, z, t)$	1·54	0·239

TABLE 1

3.5. *Surface area of the interface*

An important property of the interface which arises in connexion with the entrainment process is the surface area of the interface. For the single-valued case the surface area per unit projected area is equal to

$$\mathscr{A}' = \int_0^\infty \int_0^\infty \left[1 + \left(\frac{\partial Y}{\partial x}\right)^2 + \left(\frac{\partial Y}{\partial z}\right)^2\right]^{\frac{1}{2}} dx\, dz,$$

and its mean value is

$$\mathscr{A} = \int_0^\infty \int_0^\infty B_{Y'} \left[1 + \left(\frac{\partial Y}{\partial x}\right)^2 + \left(\frac{\partial Y}{\partial z}\right)^2\right]^{\frac{1}{2}} dx\, dz,$$

where $B_{Y'}$ is the probability density of the slope of the interface. Two problems arise with this formula: $B_{Y'}$ is inaccessible to direct measurement, and the equation holds only for single-valued $Y(x, z)$. A rather extraordinary formula for $\mathscr{A}$ has been derived by Corrsin & Phillips (1961), which overcomes both of these difficulties. It relates the mean surface area to the number of intersections made by lines drawn through the surface at different angles to the x, z plane.

Consider a straight line drawn through the point $(x, 0, z_1)$ at an angle α to the x, z plane, and whose projection onto the x, z plane makes an angle θ with the z axis (figure 7). Let $M(\alpha, \theta)$ be the mean of the number of intersections this

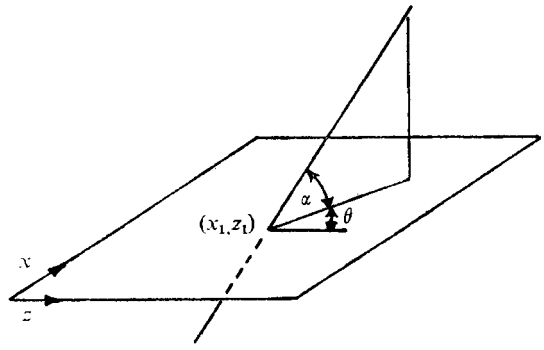

FIGURE 7. The direction for the interface crossing count.

line makes with the surface. Then Corrsin & Phillips find that the mean area of the surface per unit projected area is given by †

$$\mathscr{A} = \frac{1}{2\pi}\int_0^{2\pi}\int_0^{\frac{1}{2}\pi} M(\alpha,\theta)\sin\alpha\, d\alpha\, d\theta.$$

Further, consider the intersection of the surface with a plane which is perpendicular to the x, z plane and contains the straight line (α, θ). Then the mean contour length of this intersection per unit projected length is

$$\mathscr{L} = \int_0^{\frac{1}{2}\pi} M(\alpha,\theta)\sin\alpha\, d\alpha.$$

The quantity $M(\alpha,\theta)$ is measurable. In fact, if the rake is positioned in the direction (α,θ), the mean output of the crossing circuit would be equal to $M(\alpha,\theta)$. The rake, when tilted, was not long enough to span the interface, so traverses in the y direction were necessary to compute $M(\alpha,\theta)$. This was done for $\theta = 90°$ and $\alpha = 15°$, $30°$, $45°$, $60°$ and $90°$; and for $\theta = 0°$ and $\alpha = 0°$, $30°$, $60°$ and $90°$.

It was found that the number of crossings $K(\theta)$ per unit length of the rake was essentially independent of α and with an error of less than 7 %,

$$M(\alpha,\theta) = \int_0^{\infty} K(\theta)\, dl = \int_0^{\infty} \frac{K(\theta)}{\sin\alpha} dy$$

for $\theta = 0°$, $K(\theta) = 2{\cdot}23$ and $\theta = 90°$, $K(\theta) = 2{\cdot}36$. Since measurements at other values of θ could not be taken, it was decided to assume that $K(\theta)$ was a constant, independent of θ and equal to 2·30. Consequently, the surface area per unit projected area is given by $\mathscr{A} = 7{\cdot}2$. The mean contour lengths in the x, y $(\theta = 90°)$ and z, y $(\theta = 0°)$ planes are $\mathscr{L}_x = 3{\cdot}7$ and $\mathscr{L}_z = 3{\cdot}5$.

These extremely large values are a result of the large degree of folding of the interface. By dividing these numbers by the expected-valuedness, the contour lengths and surface area per 'value' of the interface are obtained. These give a measure of the contortion of the interface not due to folding, and are $\mathscr{A} = 3{\cdot}1$, $\mathscr{L}_x = 1{\cdot}6$, $\mathscr{L}_z = 1{\cdot}5$. The above equations for the contour length and surface area can be derived using the theory for many-valued random functions outlined in §3.3 (Lumley 1964).

† The formula of Corrsin & Phillips is incorrect.

4. Correlation measurements

4.1. *Correlations of the interface position*

An important statistical property of the interface is its space–time correlation coefficient, for this quantity provides a measure of the spatial structure of the interface and its development with time. A direct measurement of this property would require two hot-wire rakes, but, quite apart from the complexities of operating two rakes, the interference of the flow by the upstream rake would probably render this approach unfeasible. An alternative method was devised whereby space–time correlations could be constructed using the rake and a single probe.

The property whose space–time correlation will be sought is the width of the turbulent flow $H(x,z,t)$. Then

$$H(x,z,t) = \int_0^\infty I(x,y,z,t)\,dy,$$

and multiplying this by $H(x',z',t')$ and time averaging,

$$\overline{H(x'z',t')\,H(x,z,t)} = \overline{\int_0^\infty H(x',z',t')\,I(x,y,z,t)\,dy} = \int_0^\infty \overline{H(x',z',t')\,I(x,y,z,t)}\,dy.$$

The space–time covariance of $H(x,z,t)$ can thus be computed from measurements of $\overline{HI}$. Letting

$$h = H - \bar{H},$$

the correlation coefficient is

$$\mathscr{H}(\xi,\zeta,\tau) = \frac{\int_0^\infty \overline{h(x+\xi,z+\zeta,t+\tau)\,I(x,y,z,t)}\,dy}{h'(x+\xi,z+\zeta,t+\tau)\,h'(x,z,t)},$$

where the prime refers to the root-mean-square value. $\mathscr{H}(\xi,\zeta,\tau)$ will be referred to as the space–time correlation of the interface position with the understanding that if $Y(x,z,t)$ is many valued, then it is the correlation of the width of the turbulent fluid.

The rake was placed in the flow at $x/d = 360$ and a single probe with its related anemometer and detector circuit positioned upstream. This probe was traversed in the y direction, $\overline{hI}$ being computed at each y position. The rake was kept at the same place throughout, so these measurements were unconventional in the sense that the upstream probe was moved rather than the downstream probe. Since h' was not known for the single probe position, the standard deviation as computed from the intermittency factor profile was used to account for the growth of the length scales with x. The boundary-layer width and maximum mean velocity at the rake position were used to normalize ξ, ζ and τ.

To measure correlations with longitudinal separations, the single probe was displaced slightly in the z direction to minimize interference. An extrapolation of the results for a number of ζ separations showed that the effect of this displacement was negligible. In addition, the autocorrelation measurements of $h(t)$ showed that the upstream probe had no effect on the rake output. Spatial correlations with separations in the longitudinal ξ and transverse ζ directions are

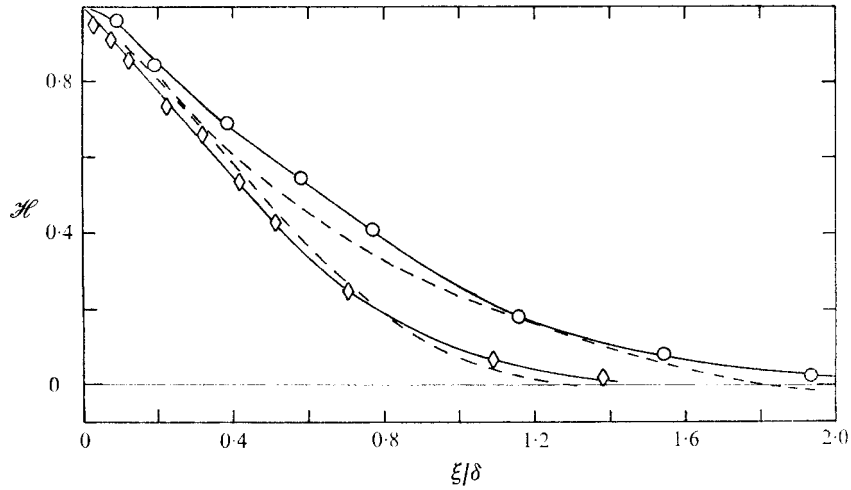

FIGURE 8. Spatial correlations of the interface position. ○, longitudinal correlation with finite separation in z direction ($\zeta_0/\delta = 0{\cdot}03$) $\mathscr{H}(\xi)$; ◇, transverse correlation $\mathscr{H}(\zeta)$; – – –, $\sin(\frac{1}{2}\pi\mathscr{H})$.

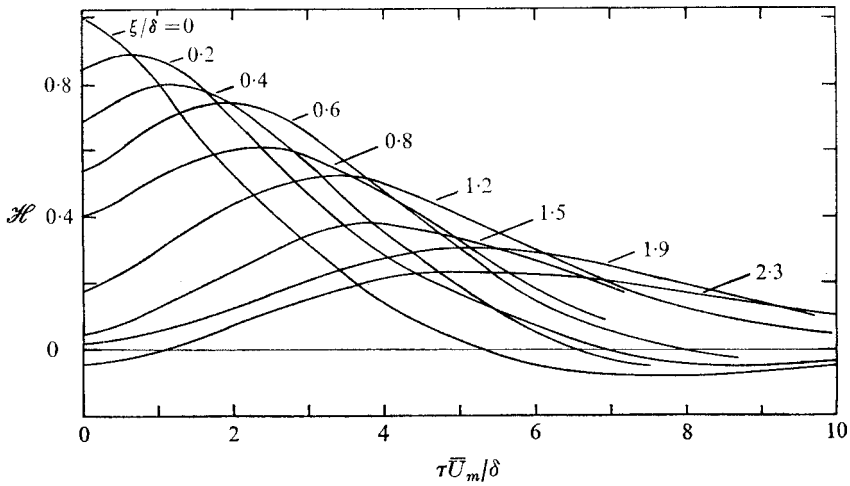

FIGURE 9. Space–time correlation of the interface position, $\mathscr{H}(\xi, \tau)$.

presented in figure 8. A characteristic length of the interface L can be defined as the separation at which the correlation falls to 0·2. The choice of this value is really arbitrary, but it does avoid the need to rely on the less accurate measurements at the lower correlation values. Thus, $\mathscr{H}(L, 0) = 0{\cdot}2$. On this basis, $L_\xi = 1{\cdot}1$, $L_\zeta = 0{\cdot}8$. It is worth noting that the measured correlations are positive for all separations. Our measurements at large separations, not shown in figure 3, confirmed this result. This is in contrast to the correlations of the interface position in a boundary-layer flow reported by Townsend (1970). These correlations were computed from films made by Fiedler & Head (1966), and show negative correlations of up to $-0{\cdot}4$. It may be that the very short averaging times necessarily used in computing these correlations are the cause of such large negative values (as noted by Townsend).

The space–time correlations of $h(x,z,t)$ shown in figure 9 exhibit a fair amount of scatter. This was due to the low time constant (20 s) of the averager in the PAR correlator used for these measurements. The space–time correlations can be characterized by two parameters: the distance D at which the envelope of the correlation curves drops to 0·2, and the time delay T at which this occurs. Thus $\partial\mathscr{H}/\partial\xi(D,T) = 0$, $\mathscr{H}(D,T) = 0{\cdot}2$. For the results presented in figure 10, $D = 1{\cdot}9\delta$, $T = 7{\cdot}4\delta/\overline{U}_m$.

The three characteristic parameters can be interpreted as follows. If there exists a dominant shape, i.e. a particular shape of the interface which makes the most significant contribution to the correlation, then it will have a size of order L and a lifetime of order T, during which time it will have moved a distance D. Of course, there is no particular reason why such a shape should exist; however, the concept is useful even if only to characterize the two-point statistics of the interface. Moreover, the visualization of free turbulent flows does hint at the existence of a preferred shape. Further support is provided by noting that the characteristic length of the correlation curves is approximately constant. This suggests that the characteristic shape maintains its form throughout its lifetime.

4.2. *The characteristic shape of the interface*

The suggestion that there may be a particular shape which characterizes the interface will be considered. Assuming for the moment that such a shape does in fact exist, it would be desirable to predict it. Properties that it should yield are the correlation functions of the interface, and the following problem is posed: given the space–time correlation $\mathscr{H}(\xi,\zeta,\tau)$, find a function $g(\xi,\zeta,\tau)$ which, when distributed randomly in space and time, will yield as its space–time correlation function $\mathscr{H}$. This problem apparently first arose in the study of shot noise (Rice 1944, 1945). The approach was applied by Townsend (1956) and Grant (1958) to predict, from velocity correlations, a shape for the large eddies of a turbulent motion by a trial and error method. Lumley (1964, 1970) presented formal methods for extracting this shape from the correlations, and it is his theory that will be used here. The correlation functions are homogeneous so the problem is greatly simplified. This approach has its limitations, for no anti-symmetrical properties of the interface can be found.

The function $h(x,z,t)$ can be expressed as

$$h(x,z,t) = \int g(x-x', z-z', t-t')\, db(x',z',t'),$$

where g is a deterministic function, db is random and

$$db(x,z,t)\, db(x',z',t') = \begin{cases} dx\, dz\, dt & \text{if} \quad (x,z,t) = (x',z',t'), \\ 0 & \text{otherwise.} \end{cases}$$

This is a decomposition of the interface into characteristic shapes $g(\xi,\zeta,\tau)$ occurring at random, uncorrelated locations and times. The Fourier–Stieltjes representation is a special case, although undesirable for it leads to a

function g which is infinite in extent. It is easily shown that, since $h(x,z,t)$ is homogeneous,

$$\mathscr{H}(\xi,\zeta,\tau) = \int g(\xi',\zeta',\tau')\, g(\xi+\xi',\zeta+\zeta',\tau+\tau')\, d\xi'\, d\zeta'\, d\tau'.$$

This equation must be solved for $g(\xi,\zeta,\tau)$; of course, the solution will not be unique, e.g. if g is a solution so is $-g$. If the Fourier transform is taken as

$$F[\mathscr{H}] = \int \mathscr{H}(\xi,\zeta,\tau) \exp\{i(k_1\xi + k_3\zeta + \omega\tau)\}\, d\xi\, d\zeta\, d\tau,$$

then, using Parseval's relation for the Fourier transform of a convolution integral

$$F[\mathscr{H}] = F[g]F^*[g],$$

where the asterisk denotes the complex conjugate. The function g can be chosen such that

$$F[g] = (F[\mathscr{H}])^{\frac{1}{2}}, \quad \text{i.e.} \quad g = F^{-1}[(F[\mathscr{H}])^{\frac{1}{2}}].$$

As an example consider the simple case where

$$\mathscr{H}(\xi) = \exp\{-\xi^2/\lambda^2\}.$$

Then

$$F[\mathscr{H}] = \lambda\pi^{\frac{1}{2}} \exp\{-\tfrac{1}{2}\lambda^2 k_1^2\} \quad \text{and} \quad g(\xi) = (4/\pi)^{\frac{1}{4}} \exp\{-2\xi^2/\lambda^2\}.$$

The characteristic shape has the same form as the correlation function but has a more rapid decay.

To determine the characteristic shape for any interface a complete description of the space–time correlation is required. Since our results are insufficient, we must be satisfied with something less than the complete shape. A function $g(\xi)$ will be sought which, when distributed along the x axis at random uncorrelated positions, will have for its correlation function $\mathscr{H}(\xi)$. The same will be done for the transverse direction. Guided by the simple example above, we can expect the characteristic shape to be similar in shape to the correlation function, but narrower. To the spatial correlations in figure 8, expressions of the form

$$\exp\{-a\xi^2\} \sum_{n=0}^{3} b_n \xi^{2n}$$

were fitted by a least-squares method. These expressions were then used to calculate g by digital computation, and the results are shown in figure 10. As shown they would represent a characteristic 'bulge' of the interface; inverted they would typify a 'valley'. It is necessary to question the meaning of this characteristic shape of the interface. What is its significance? If the interface were frozen at any instant and observed, would this shape be apparent? The density of the distribution of shapes (i.e. the mean number occurring per unit length) is arbitrary in the sense that any density will yield the same correlation function. If this density is low and the shapes are spaced far apart, then they should be observable, if they exist. If spaced so close that they interact, then they might not be apparent. The extent of $g(\xi)$ is about $1{\cdot}5\delta$, so this would represent the closest spacing possible before the shapes interact. Consequently,

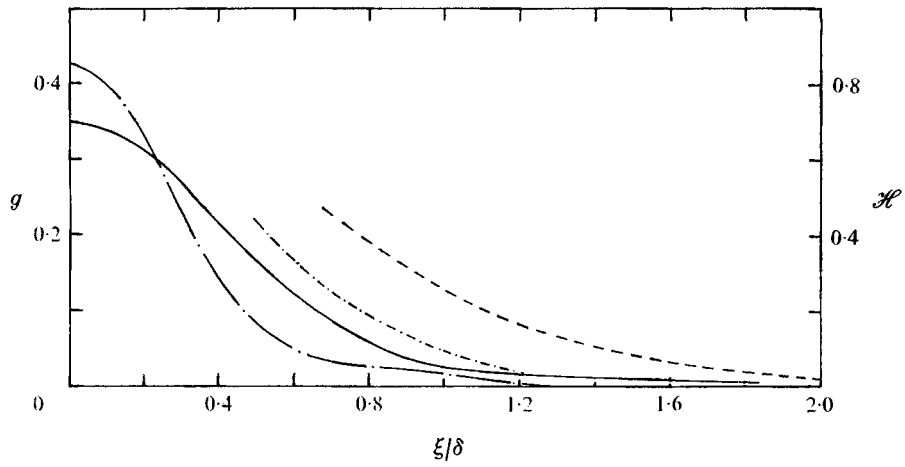

FIGURE 10. Characteristic shapes for the interface. ——, longitudinal shape $g(\zeta)$; —·—, transverse shape $g(\zeta)$; – – – –, $\mathscr{H}(\xi)$; –·–·–, $\mathscr{H}(\zeta)$.

if there is to be no interaction between characteristic shapes, the mean number of crossings of the interface per unit length should be less than $M_x = 2/1{\cdot}5\delta = 1{\cdot}3\delta^{-1}$. However, our measurements indicate that $M_x = 3\delta^{-1}$, so such a large spacing is unlikely. To resolve this question, some detailed visualization of the flow would be necessary. It is on this basis that Townsend (1966) has proposed a periodic type of structure for the interface in a wake flow. Such periodicities have not appeared in any correlation measurements in any flow. It is important to note that the existence of a characteristic shape in no way implies a periodic structure.

4.3. *Convection velocity of the interface*

A convection velocity of the interface in the x direction is conveniently defined as

$$\mathscr{C}'_x = -\frac{\partial Y}{\partial t}\Big/\frac{\partial Y}{\partial x}. \tag{2}$$

This definition can be motivated a number of ways. If the interface is represented as

$$x = X(y,z,t),$$

then (Phillips 1972)

$$\mathscr{C}'_x = \partial X/\partial t.$$

Longuet-Higgins (1956, 1957) showed that (2) gives the velocity of intersections of the interface with a line parallel to the x axis, and this type of method has been used by Kovasznay *et al.* (1970) to estimate convection velocities. For the special case where $Y(x,z,t)$ is a Gaussian variable whose derivatives are also Gaussian, the mean value of the convection velocity is

$$\mathscr{C}_x = \overline{\frac{\partial Y}{\partial t}\frac{\partial Y}{\partial x}}\Big/\left(\overline{\frac{\partial Y}{\partial x}}\right)^2, \tag{3}$$

and is independent of the location of the line drawn through the surface (Longuet-Higgins 1956, 1957). In general, no simple form for the mean convection velocity

can be derived. This is unfortunate, for it is desirable to have a convection velocity that can be computed from the space–time correlations of $h(x, z, t)$. Consequently, (3) will be taken as the definition of the convection velocity, and it will be shown that it is derivable from the space–time correlation of $h(x, z, t)$.

A number of convection velocities can be defined from the space–time correlations. For a given probe spacing the ratio of this spacing to the time delay required for a maximum in the correlation curve defines one convection velocity, $\mathscr{C}_\xi$ say. This is given by the slope of the locus of all points in the ξ, τ plane at which $\partial\mathscr{H}/\partial\tau = 0$. So

$$\mathscr{C}_\xi = -\frac{\partial^2\mathscr{H}}{\partial\tau^2}\Big/\frac{\partial^2\mathscr{H}}{\partial\xi\,\partial\tau},$$

and, since $\mathscr{C}_\xi$ will in general vary with ξ or τ, its value for $\xi = \tau = 0$ will be used.

An alternative procedure is to compute for a given time delay the separation required to achieve maximum correlation. The convection velocity $\mathscr{C}_\tau$ is defined as the ratio of this probe separation to the given time delay. This latter definition seems better for one prefers to treat the complete flow field at specific instances rather than time records at particular points. Unfortunately, it is the former that is more easily determined.

The convection velocity $\mathscr{C}_\tau$ can be found from the envelope of the curves in figure 9, and because it is characterized by the condition $\partial\mathscr{H}/\partial\xi = 0$, it is given by

$$\mathscr{C}_\tau = -\frac{\partial^2\mathscr{H}}{\partial\xi\,\partial\tau}\Big/\frac{\partial^2\mathscr{H}}{\partial\xi^2}.$$

The two convection velocities just defined are analogous to the celerities of Favre, Gaviglio & Dumas (1967). $\mathscr{C}_\tau$ also varies with ξ and τ, and the value corresponding to $\xi = \tau = 0$ will be used. It is easily shown that, if $Y(x, z, t)$ is a homogeneous function of x, then

$$\mathscr{C}_\xi = -\overline{\left(\frac{\partial Y}{\partial t}\right)^2}\Big/\overline{\frac{\partial Y}{\partial x}\frac{\partial Y}{\partial t}}$$

and

$$\mathscr{C}_\tau = -\overline{\frac{\partial Y}{\partial x}\frac{\partial Y}{\partial t}}\Big/\overline{\left(\frac{\partial Y}{\partial x}\right)^2}.$$

The convection velocities were estimated from the curves in figure 9, and it was found that

$$\mathscr{C}_\xi = 0{\cdot}30\overline{U}_m, \quad \mathscr{C}_\tau = 0{\cdot}19\overline{U}_m. \tag{4), (5}$$

The mean velocity varies from approximately $0{\cdot}32\overline{U}_m$ to $0{\cdot}05\overline{U}_m$ over the intermittent region and is equal to $0{\cdot}15\overline{U}_m$ at $\overline{Y}$.

An alternative method was used to estimate a convection velocity. The rake was aligned parallel to the x axis at $\overline{Y}$, the mean output of the crossing circuit was measured, and the average number of interface crossings per unit length was calculated. Next, the average number of crossings per unit time was measured using a single probe. This is twice the interface crossing rate. The two values obtained were, respectively,

$$M_x = 3{\cdot}0\delta^{-1}, \quad M_t = 0{\cdot}45\overline{U}_m/\delta. \tag{6}$$

The ratio of these two numbers defines a convection velocity

$$\mathscr{C}_m = M_t/M_x = 0{\cdot}15\overline{U}_m. \tag{7}$$

This method is much the same as that used by Kovasznay *et al.* (1970). It should be emphasized that convection velocities determined in this way are theoretically unsound. They are determined by essentially timing the passage of the interface across a fixed distance d, between two probes. Let the time of passage for the ith crossing of the interface be Δt_i. Then the measured convection velocity averaged over N crossings is

$$\mathscr{C}_M = Nd \Big/ \sum_{i=1}^{N} \Delta t_i.$$

However, the convection velocity for the ith crossing is

$$\mathscr{C}_i = d/\Delta t_i,$$

and the mean convection velocity for N crossings is

$$\mathscr{C} = N^{-1} \sum_{i=1}^{N} \mathscr{C}_i = N^{-1} d \sum_{i=1}^{N} (1/\Delta t_i).$$

Now it is easily shown from the Cauchy–Schwarz inequality that

$$N \Big/ \sum_{i=1}^{N} \Delta t_i \leqslant N^{-1} \sum_{i=1}^{N} (1/\Delta t_i),$$

therefore

$$\mathscr{C}_M \leqslant \mathscr{C}, \tag{8}$$

so this estimate of the convection velocity will be too low. This is indeed so for the present measurements (cf. (6) and (7)).

Using the interface crossing technique, Kovasznay *et al.* found that, for the turbulent boundary layer, the overall convection velocity was $0{\cdot}93\overline{U}_\infty$, where $\overline{U}_\infty$ is the free-stream velocity. The convection velocity estimated from their space–time correlations of the intermittency function is $0{\cdot}96\overline{U}_\infty$† (table 2). Therefore, for these experiments, the difference in the values obtained by the two methods are within the accuracy of the data and are not inconsistent with the prediction of (8).

4.4. *The slope of the interface*

In the light of the discussion of the many-valuedness of the interface position, the slope will also be many-valued and will at times be infinite. It is reasonable to assume that the turbulent flow is a simply-connected region, so the interface does not touch itself at any time. Consequently, the expected-valuedness of the slope will be the same as for the interface position.

The theory of Lumley could be applied to the study of the statistical properties of the interface slope. However, no direct measure of the slopes of the interface was available so this approach would not be fruitful. Properties of the derivatives of the width of the turbulence $H(x, z, t)$ can be found, and these will be considered, with the knowledge that the results will apply to the interface position, if it is single-valued.

† Blackwelder has estimated $0{\cdot}94\overline{U}_\infty$.

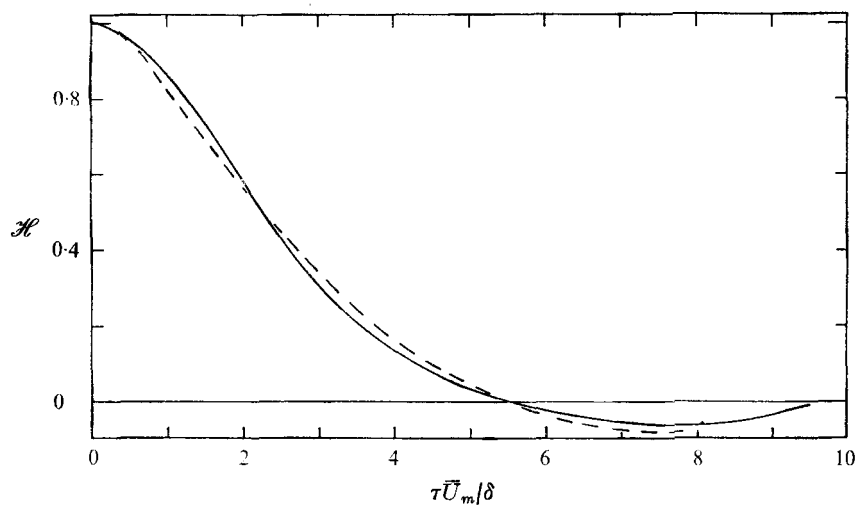

FIGURE 11. Autocorrelation of the interface position.
——, $\mathscr{H}(\tau)$; – – – –, sin $(\frac{1}{2}\pi\mathscr{H})$.

Since $h(t)$ was available at the output of the summing amplifier, it was hoped that by simply differentiating this output the r.m.s. value of $h(t)$ could be found. Unfortunately, since h was not a continuous signal, differentiating the signal produced spikes, which could not be filtered out without significantly affecting the signal. From the autocorrelation of $h(t)$ (figure 11), a microscale μ can be determined. This is related to the time rate of change of h by

$$(\partial h/\partial t)' = \sqrt{2}h'/\mu,$$

where the primes refer to the r.m.s. value. To relate the time derivative of h to its spatial derivative a convection velocity is needed. Which to use follows easily from

$$\overline{\left(\frac{\partial h}{\partial t}\right)^2}\Big/\overline{\left(\frac{\partial h}{\partial x}\right)^2} = \frac{\partial^2\mathscr{H}(0)}{\partial\tau^2}\Big/\frac{\partial^2\mathscr{H}(0)}{\partial\xi^2} = \mathscr{C}_\tau\mathscr{C}_\xi.$$

The value of μ was estimated from the autocorrelation curve as $\mu = 2{\cdot}24\delta/\bar{U}_m$. Using the value 2·4 for h' (§3.4), $(\partial h/\partial t)' = 0{\cdot}15\bar{U}_m$, and using (5) and (6) for the convection velocities, $(\partial h/\partial x)' = 0{\cdot}64$. From the spatial correlation $\mathscr{H}(\xi)$ a microscale λ_ξ can be estimated as $\lambda_\xi = 0{\cdot}45$, and this leads to an r.m.s. slope of $(\partial h/\partial x)' = 0{\cdot}75$. The agreement is satisfactory.

The spatial derivative of the width of the turbulent flow could be used as an estimate of the slope of the surface; however, owing to folding, the estimate will always be too low. Some idea of the surface slope can be obtained from the interface crossing rate M_x. Using the Rice–Kac zero-crossing formula for Gaussian variables (Rice 1944, 1945),

$$M_x = \frac{1}{\pi\sigma}\left(\frac{\partial Y}{\partial x}\right)'.$$

Using the value (6) for M_x and $\sigma = 0{\cdot}3\delta$, $(\partial Y/\partial x)' = 2{\cdot}8$. Dividing by the expected-valuedness to give a slope per value of Y, $(\partial Y/\partial x)' = 1{\cdot}2$. This is twice the value

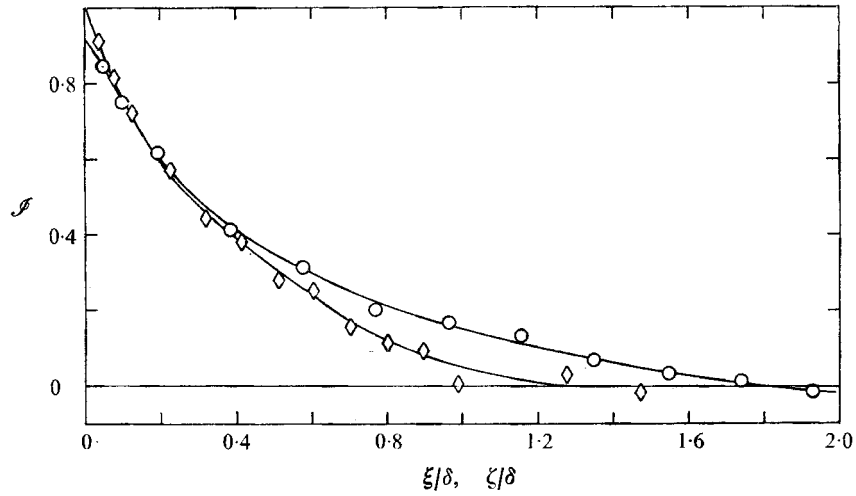

FIGURE 12. Spatial correlations of the intermittency function. ○, longitudinal correlation with finite separation in z direction ($\zeta_0/\delta = 0{\cdot}03$) $\mathscr{I}(\xi)$; ◇, transverse correlation $\mathscr{I}(\zeta)$.

obtained for the spatial derivative of h and it is a bit surprising that it is not greater, since the slope of Y must be infinite every time a fold occurs. In fact, the r.m.s. value of the slope of Y could be infinite. Corrsin & Phillips (1961) derived a formula for the contour length of a single-valued Gaussian variable. The formula is of the form

$$\mathscr{L} = f(\sigma),$$

where f is a rather complicated function. Using the r.m.s. slope per value of 1·2 yields a contour length of 1·5, which compares favourably with that reported in § 3.5.

4.5. *Space–time correlations of the intermittency function*

The space–time correlations of the intermittency function $I(x, y, z, t)$ were also measured. The idea was to see how much information about the interface could be gained with just these measurements, for they are far more easily obtained than the correlations of the interface position.

The probe in the rake which was closest to the mean position of the interface was used as the fixed probe and the movable probe was the same as that used in the $\overline{hI}$ measurements. This probe was kept close to the mean position of the interface for all measurements. The correlation coefficient measured was

$$\mathscr{I}(\xi, \zeta, \tau) = \frac{\overline{i(x+\xi, \overline{Y}, z+\zeta, t+\tau)\, i(x, \overline{Y}, z, t)}}{i'(x+\xi, \overline{Y}, z+\zeta, t+\tau) i'(x, \overline{Y}, z, t)},$$

where

$$i = I - \bar{I}.$$

It is easily shown that

$$i'^2 = \overline{i^2} = \bar{I}(1-\bar{I}).$$

Spatial correlations $\mathscr{I}(\xi)$ and $\mathscr{I}(\zeta)$ are shown in figure 12. Here the effect of the transverse displacement of the probe was significant. The space–time correlations are presented in figure 13. There is some similarity in these sets of curves and the correlations of interface position; however, the latter are substantially

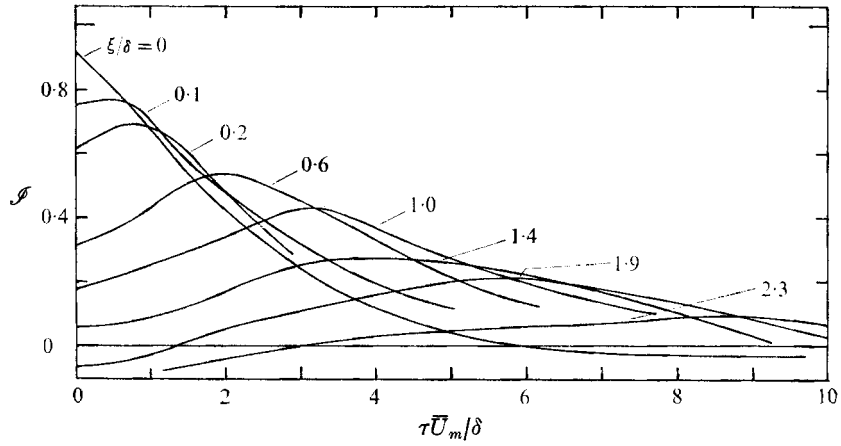

FIGURE 13. Space–time correlations of the intermittency function $\mathscr{I}(\xi, \tau)$.

	Wall jet				Boundary layer†	
	$\mathscr{H}$	$\mathscr{I}$	$R_{11}(\overline{Y})$	$R_{11}(\delta)$	$\mathscr{I}$	$R_{11}(\overline{Y})$
L_ξ/δ	1·1	0·83	1·1	1·05	0·5	0·7
L_τ/δ	0·8	0·66	—	—	0·31	—
L_ξ/L_ζ	1·4	1·3	—	—	1·6	—
D/δ	1·9	1·4	1·4	3·0	8·7	10·0
$T\overline{U}_m/\delta$	7·4	6·0	6·5	4·8	9·0	10·5
$\mathscr{C}_\xi/\overline{U}_m$	0·30	0·27	—	0·63	0·96	0·92
$\mathscr{C}_\tau/\overline{U}_m$	0·19	0·16	—	0·48	0·96	0·92

† Results of Blackwelder & Kovasznay (1972*b*) and Kovasznay *et al.* (1970).

TABLE 2. Properties of space–time correlation functions.

broader than those of the intermittency function. This is reflected in the smaller scales derived from the intermittency function (table 2). Also tabulated are the convection velocities, computed in the same way as for the interface position. The convection velocity $\mathscr{C}_\tau$ is approximately equal to the mean velocity at $\overline{Y}$.

If it is assumed that $h(x, z, t)$ is a Gaussian variable, then its correlation is uniquely related to that of $I(x, \overline{Y}, z, t)$ by (Corrsin & Kistler 1955; Papoulis 1965)

$$\mathscr{H} = \sin(\tfrac{1}{2}\pi\mathscr{I}). \tag{9}$$

This formula was applied to the longitudinal, transverse and autocorrelations of the intermittency function and the results are compared with the corresponding correlations of interface position in figures 8 and 12. The agreement is good, the worst case being the longitudinal correlations: this may be due to the probe interference. Without knowledge of the correlations of h, (9) represents a very good estimate of $\mathscr{H}$, certainly better than using $\mathscr{I}$ alone.

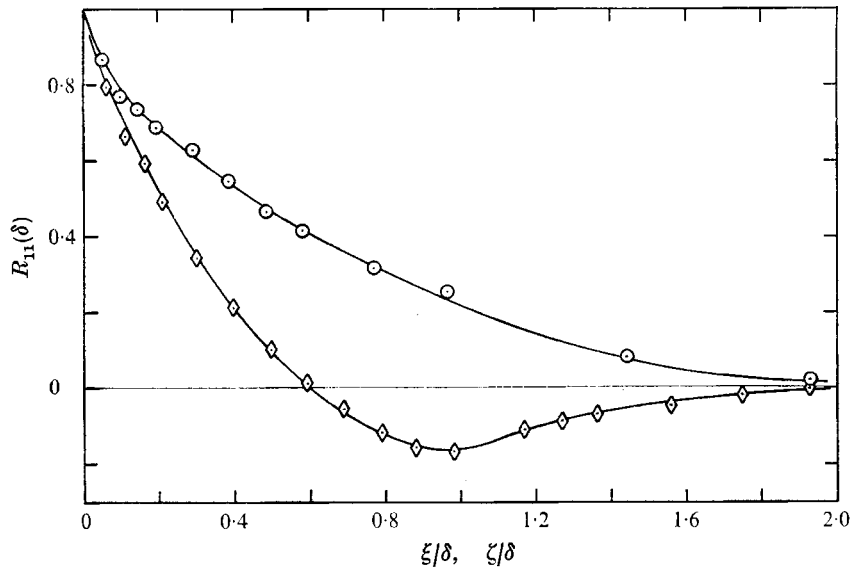

FIGURE 14. Spatial correlations of velocity at δ. ○, longitudinal correlation $R_{11}(\xi;\delta)$; ◇, transverse correlation $R_{11}(\zeta;\delta)$.

4.6. *The turbulent motion in the intermittent region*

The measurements of Kovasznay *et al.* (1970) (also Blackwelder & Kovasznay 1972*b*) confirmed the widely held view that the behaviour of the interface should be intimately related to the large-scale turbulent motion occurring in the neighbourhood of the interface. A similar, although less detailed, confirmation for the wall jet was made by measurements of correlations of the longitudinal components of velocity

$$R_{11}(\xi,\eta,\zeta,\tau;y_0) = \frac{\overline{u(x+\xi,y_0+\eta,z+\zeta,t+\tau)\,u(x,y_0,z,t)}}{\overline{u'(x+\xi,y_0+\eta,z+\zeta,t+\tau)\,u'(x,y_0,z,t)}}.$$

To characterize the fully turbulent region, spatial correlations with longitudinal and transverse separations, and space–time correlations with longitudinal separations were measured with both probes maintained at one boundary-layer thickness from the wall. These measurements were repeated with the probes maintained at $y_0 = \overline{Y}$ to characterize the flow in the intermittent region. The results are collected in figures 14–17. The longitudinal correlations of u are almost identical at the two locations while the transverse correlations differ markedly, the familiar negative portion of the correlation at δ being almost non-existent at $\overline{Y}$. Also, the scale of the transverse motion is much smaller at δ.

The space–time correlations at δ and $\overline{Y}$ differ; the latter resemble those of h and I, while the former show a quite rapid decay. The characteristic parameters are assembled in table 2. The length scales L_ξ are not shown for the transverse separations. These correlations differ in shape from those of h and I, so the length scales would not have the same significance. Also presented are the convection velocities for the correlations at δ (those at $\overline{Y}$ had too much scatter to make

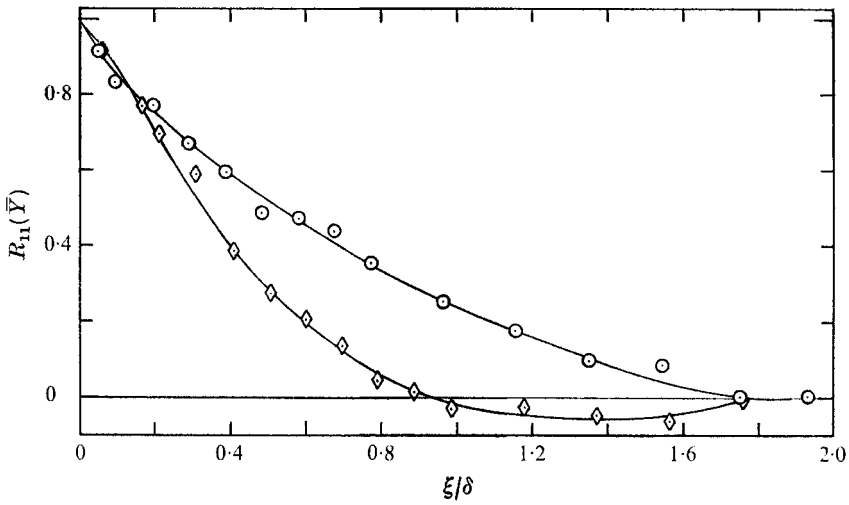

FIGURE 15. Spatial correlations of velocity at $\bar{Y}$. ⊙, longitudinal correlation $R_{11}(\xi; \bar{Y})$; ◇, transverse correlation $R_{11}(\zeta; \bar{Y})$.

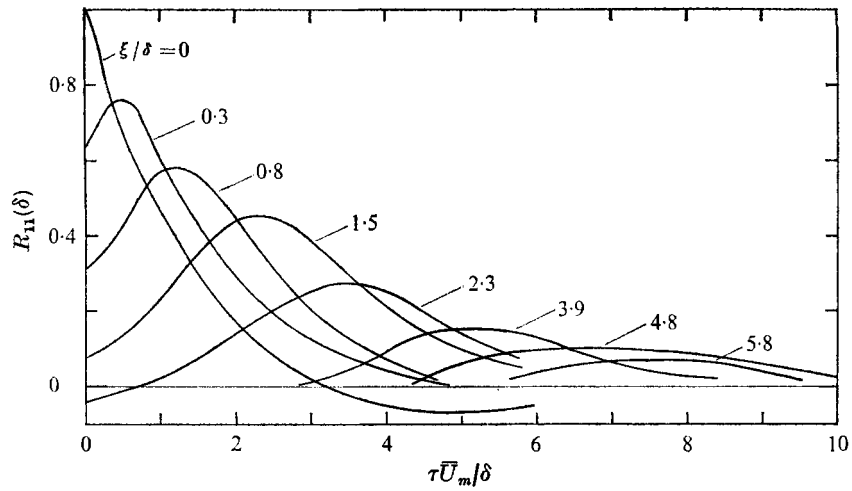

FIGURE 16. Space–time correlations of velocity at δ, $R_{11}(\xi, \tau; \delta)$.

quantitative estimates). These were computed in the manner described previously and compare rather favourably with the convection velocities measured in a round jet by Wygnanski & Fiedler (1969). The convection velocity $\mathscr{C}_\tau$ is almost equal to the local mean velocity.

Finally, spatial correlations with separation in the inhomogeneous y direction were measured with the fixed probe at $\bar{Y}$. A displacement of the movable probe in the z direction was necessary, to traverse past the fixed probe. These measurements are shown in figure 18, together with the intermittency factor profile. The extent of correlation is almost identical to the range of the interface position, again showing up this intimate connexion between the turbulent motion and the interface.

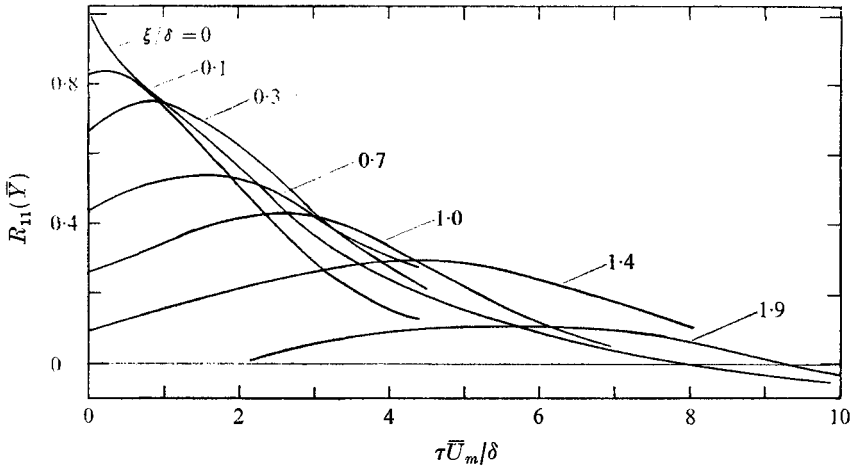

FIGURE 17. Space-time correlations of velocity at $\bar{Y}$, $R_{11}(\xi, \tau; \bar{Y})$.

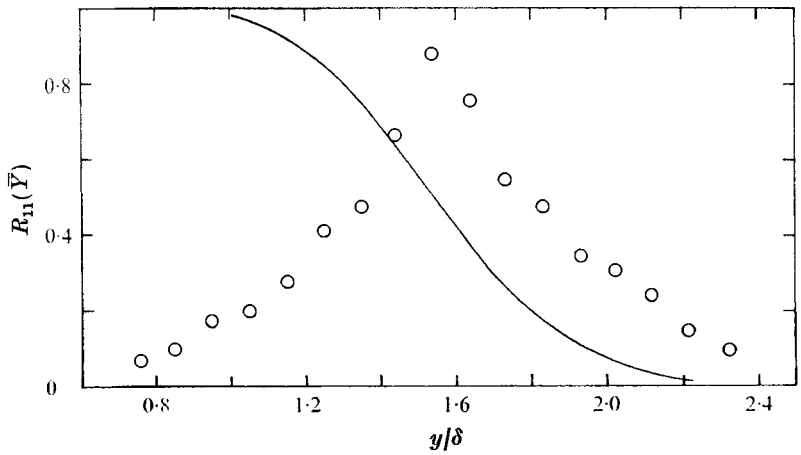

FIGURE 18. Spatial correlations of velocity. ○, correlation with finite separation in z direction ($\zeta_0/\delta = 0{\cdot}05$) $R_{11}(\eta; \bar{Y})$; ——, $\bar{I}$.

The turbulent velocity field of a wall jet has been the subject of detailed studies by Hodgson (1972, private communication) and Mathieu (1971). The few correlation measurements presented here are in reasonable agreement with their results.

4.7. *Comparison with the turbulent boundary layer*

The results presented in this section can be taken as representative of jet flows, and it is worth comparing them with the results of Blackwelder & Kovasznay (1972*b*) and Kovasznay *et al.* (1970) for the boundary layer with zero pressure gradient. They measured space–time correlations of I, u, v and uv, and found that they persisted over very large distances downstream. Equivalent scales have been calculated for their correlations of u and I, and are included in table 1. The length scales of the spatial correlations for the boundary layer are appreciably smaller than those for the wall jet and the ratio of the scales shows that the shape of the interface in the boundary layer is slightly more elongated in the x direction.

The persistence of the space-time correlations for the boundary layer is primarily a result of the large convection velocities, since the ratio of the decay times T is 1·5, as compared with the ratio of distances D, which is about 6. Thus, the lifetimes of the characteristic shapes are of the same order of magnitude in the two flows.

5. Conclusions

A study of the geometrical properties of the interface in a turbulent wall jet using a multiple array of turbulence detector probes reveals a highly contorted interface shape, which is distinctly three-dimensional. The contortion is so great that the interface position, expressed as the height of the interface from the wall, is multiple-valued for as much as 40 % of the time. However, the quantity of turbulent fluid carried in the folded regions is small, about 10 % of the turbulent fluid in the intermittent region.

Using a theory of Lumley (1964, 1970) to study the statistical properties of such surfaces, the degree of contortion can be characterized by the expected-valuedness, which gives the average number of values taken on by the interface position. This was found to be 2·35 (for single-valued functions it is of course unity). The most significant aspect of this many-valued nature of the interface is that it leads to extremely large surface areas. This property was measured in the wall jet flow using a formula of Corrsin & Phillips (1961), and it was found that the ratio of surface area to projected area was 7·2. Thus, in dealing with properties that involve the slope of the interface, it is important to take note of this feature of the interface. Studies of other shear flows suggest that this phenomenon is a property of all interfaces.

The close agreement between the probability distribution of the interface and the intermittency factor profile allows one to overlook the many-valued character of the interface when dealing with global features of the interface. This is no doubt due to the fact that so little turbulence is carried by the folded regions. Measurements of space and space–time correlations of the total width of the turbulent fluid have been performed, and estimates of scales of sizes and decay times based on these results have been made. It is concluded that a typical shape of the interface has a length in the longitudinal direction approximately equal to the boundary-layer width δ, and a transverse width of $0{\cdot}8\delta$. Taking the height of this shape as the standard deviation, $\sigma = 0{\cdot}3\delta$, the aspect ratio is 0·3. In the light of the above discussion, this cannot be related to the slope of the interface. The decay time of this shape is $7{\cdot}4\delta/\overline{U}_m$, and the distance travelled during this time is 2δ. This is in contrast to the situation in a boundary layer where (Kovasznay *et al.* 1970) the decay times are of the same order, but owing to the larger velocity in the vicinity of the interface, the distance traversed by the typical shape is about ten boundary-layer thicknesses. Following a method of Lumley (1964, 1970), a characteristic shape of the interface has been formally deduced from the spatial correlations. This has much the same properties although it has a smaller height than given above. The question of a convection velocity of the interface has been examined, and a suitable convection velocity has been

defined, which can be calculated from the space–time correlations. This yields a value close to the mean velocity at the mean position of the interface.

The financial assistance of the South African Council for Scientific and Industrial Research is gratefully acknowledged. This study was supported by the National Science Foundation under grant GK 10470.

REFERENCES

BLACKWELDER, R. F. & KOVASZNAY, L. S. G. 1972*a* *J. Fluid Mech.* **53**, 61.

BLACKWELDER, R. F. & KOVASZNAY, L. S. G. 1972*b* *Phys. Fluids*, **15**, 1545.

COLES, D. & VAN ATTA, C. W. 1967 *Phys. Fluids Suppl.* **10**, 120.

CORRSIN, S. 1943 *N.A.C.A. Wartime Rep.* W-94.

CORRSIN, S. & KISTLER, A. L. 1955 *N.A.C.A. Rep.* no. 1244.

CORRSIN, S. & PHILLIPS, O. M. 1961 *J. Soc. Indust. Appl. Math.* **9**, 395.

FAVRE, A., GAVIGLIO, J. & DUMAS, R. 1967 *Phys. Fluids Suppl.* **10**, 138.

FIEDLER, H. & HEAD, M. R. 1966 *J. Fluid Mech.* **25**, 719.

GRANT, H. L. 1958 *J. Fluid Mech.* **4**, 149.

HEAD, M. R. 1958 *Aero. Res. Counc. R. & M.* no. 3152.

KAPLAN, R. E. & LAUFER, J. 1969 *Proc. 12th Int. Cong. on Appl. Mech.*, p. 236. Springer.

KOHAN, S. M. 1968 Ph.D. dissertation, Stanford University.

KOVASZNAY, L. S. G. 1971 *AGARD-CP-93.*

KOVASZNAY, L. S. G., KIBENS, V. & BLACKWELDER, R. F. 1970 *J. Fluid Mech.* **41**, 283.

LONGUET-HIGGINS, M. S. 1956 *Proc. Camb. Phil. Soc.* **52**, 234.

LONGUET-HIGGINS, M. S. 1957 *Phil. Trans.* A **249**, 321.

LUMLEY, J. L. 1964 *J. Math. Phys.* **5**, 1198.

LUMLEY, J. L. 1970 *Stochastic Tools in Turbulence, Academic.*

LUNDGREN, T. S. 1970 On the structure of the turbulent interface. *Boeing Symp. on Turbulence.*

MATHIEU, J. 1971 *Von Kármán Institute for Fluid Dynamics, Lecture Series* 36.

MOBBS, F. R. 1967 *J. Fluid Mech.* **33**, 227.

MOFFATT, H. K. 1965 *Stanford University, SUDAER* 242.

NEE, V. W. & KOVASZNAY, L. S. G. 1969 *Phys. Fluids*, **12**, 473.

PAIZIS, S. T. 1972 Ph.D. dissertation, The Johns Hopkins University.

PAPOULIS, A. 1965 *Probability, Random Variables, and Stochastic Processes.* McGraw-Hill.

PHILLIPS, O. M. 1955 *Proc. Camb. Phil. Soc.* **51**, 220.

PHILLIPS, O. M. 1972 *J. Fluid Mech.* **51**, 97.

REYNOLDS, W. C. 1972 *J. Fluid Mech.* **54**, 481.

RICE, O. 1944 *Bell Syst. Tech. J.* **23**, 282.

RICE, O. 1945 *Bell Syst. Tech. J.* **24**, 46.

SAFFMAN, P. G. 1970 *Proc. Roy. Soc.* A **317**, 417.

SCHWARZ, W. H. & COSART, W. P. 1961 *J. Fluid Mech.* **10**, 418.

TOWNSEND, A. A. 1948 *Australian J. Sci. Res.* **1**, 161.

TOWNSEND, A. A. 1949 *Australian J. Sci. Res.* **2**, 451.

TOWNSEND, A. A. 1956 *The Structure of Turbulent Shear Flow.* Cambridge University Press.

TOWNSEND, A. A. 1966 *J. Fluid Mech.* **26**, 689.

TOWNSEND, A. A. 1970 *J. Fluid Mech.* **41**, 13.

WYGNANSKI, I. & FIEDLER, H. E. 1969 *J. Fluid Mech.* **38**, 577.

WYGNANSKI, I. & FIEDLER, H. E. 1970 *J. Fluid Mech.* **41**, 327.